Membrane Topology and Omeprazole Labeling of the Gastric H^+,K^+-Adenosinetriphosphatase†

Marie Besancon,‡ Jai Moo Shin,‡ Frederic Mercier,‡ Keith Munson,‡ Melissa Miller,§ Steve Hersey,§ and George Sachs*,§

Departments of Physiology and Medicine, University of California—Los Angeles, and Wadsworth Veterans Affairs Hospital, Los Angeles, California 90073, and Department of Physiology, Emory University, Atlanta, Georgia 30322

Received August 28, 1992; Revised Manuscript Received December 8, 1992

ABSTRACT: The gastric H^+,K^+-ATPase is an $\alpha\beta$ heterodimer with close homology to the Na^+,K^+-ATPase. Digestion of intact cytoplasmic-side-out vesicles at a trypsin to protein ratio of 1/4 removed most of the cytoplasmic protein, leaving membrane-spanning pairs in high yield. These were visualized on gels and poly(vinylidene difluoride) (PVDF) membranes by sodium dodecyl sulfate solubilization of the membrane-embedded segments and labeling of the cysteine residues with fluorescein maleimide prior to electrophoresis. The membrane-spanning residues of the α subunit were found between positions 104 and 162 (M1/M2), 291 and 358(M3/M4), 776 and 835(M5/M6), and 853 and 946(M7/M8). Although this method did not detect membrane retention of the hydrophobic sequences subsequent to position 946, it provided biochemical evidence for at least eight membrane segments in the catalytic subunit. Intact vesicles containing this enzyme transport acid in the presence of KCl, valinomycin, and MgATP. Omeprazole accumulates in these acidified vesicles and converts to a cationic sulfenamide. This forms disulfides with accessible cysteines. The reaction with this extracytoplasmic thiol reagent inhibits ATPase activity. Full inhibition was obtained with a stoichiometry of 2.2 mol of omeprazole bound/mg of protein. Only the α subunit was labeled. The cysteines reacting with omeprazole were defined by proteolytic cleavage of ^3H- or ^{14}C-omeprazole-labeled enzyme followed by peptide sequencing of fragments separated on tricine gradient gels and transferred to PVDF membranes. Tryptic digestion at a 1/40 trypsin to protein ratio in the presence of ligands that stabilize the E_2P form of the enzyme produced two large fragments, one of 68 kDa stretching from Glu^{47} to probably Arg^{666} that contained minor labeling and the other of 33 kDa beginning at Ala^{671} and extending to probably Arg^{946} that contained greater than 85% of the label. Digestion of labeled vesicles at 1/75 or 1/4 trypsin to protein ratios gave radioactive patterns consistent with labeling at Cys^{813} and/or Cys^{822} and at Cys^{892} and/or Cys^{927} and/or Cys^{938}. V8 protease digestion of the solubilized α subunit produced a fragment extending from Ser^{838} to possible Asp^{900} that was omeprazole-labeled, showing that Cys^{892} was labeled and Cys^{927} and Cys^{938} were not. Hence, omeprazole labels the H^+,K^+-ATPase at cysteines within the M5/M6 and M7/M8 regions of the α subunit, accounting for its inhibitory action in vivo and in vitro.

The gastric H^+,K^+-ATPase is a member of the ion-motive, phosphorylating class of transport ATPases which includes the Na^+,K^+-, Ca^{2+}, and H^+-ATPases. This enzyme catalyzes an electroneutral exchange of extracytoplasmic K^+ for cytosolic H_3O^+ (Sachs et al., 1976). The H^+,K^+-ATPase consists of an α,β heterodimer (Hall et al., 1991) similar to the Na^+,K^+-ATPase. These two ion pumps show striking primary sequence homology, 75% in the case of the α_1 subunit (Maeda et al., 1988; Shull & Lingrel, 1986) and 35% in the case of the β_2 subunits of the sodium pump as compared to the subunits of the H^+,K^+-ATPase (Reuben et al., 1990; Shull, 1990). For both of these pumps the catalytic cycle involves ATP and ionic-ligand-dependent changes in conformation which result in cyclic alteration of binding-site affinity and transmembrane ion movement.

Despite our present knowledge of the catalytic cycles and primary structures, the molecular mechanism whereby the scalar energy of ATP is converted to vectorial ion transport remains elusive. Since ion movement must occur across the membrane domain of the pump, knowledge of the secondary structure of the membrane domain is an initial step in analysis of the ion pathway. The most common approach to defining membrane-spanning segments is by means of hydropathy plots. While a useful technique, such analysis of certain regions, especially in the C-terminal one-third of the catalytic subunit of EP-type pumps, gives ambiguous results. Determination of the membrane-spanning segments of these pumps requires confirmation of the predictions by more direct methods.

One method is to define protease-sensitive sites in the intact cytoplasmic-side-out vesicles of the H^+,K^+-ATPase obtained routinely from hog gastric mucosa (Sachs et al., 1976). Here, tryptic cleavage of the α subunit in such vesicles at a 1/4 trypsin to protein ratio followed by fluorescein maleimide labeling of membrane-retained cysteines provided evidence for four pairs of membrane-spanning segments, corresponding to the first four pairs predicted for the Ca^{2+}-ATPase (MacLennan et al., 1985; Matthews et al., 1990). No evidence for the last pair predicted from hydropathy was obtained by this technique. Also, no evidence was obtained for cleavage of the β subunit under these conditions, suggesting that most of the tryptic cleavage sites for this subunit were extracytoplasmic.

Another way of determining secondary structure involved in transport is to define the binding sites for extracytoplasmic

† Supported by U.S. Veterans Affairs SMI and NIH Grants DK 40615, 41301, and 14752. Sequencing of the peptides was supported by NIH BRS Shared Instrumentation Grant 1S10RR0554-01 to UCLA and was kindly performed by Dr. Audree Fowler. J.M.S. was supported in part by a postdoctoral fellowship from Merck Sharp and Dohme.

* To whom correspondence should be addressed.
‡ UCLA and Wadsworth VA Hospital.
§ Emory University.

0006-2960/93/0432-2345$04.00/0

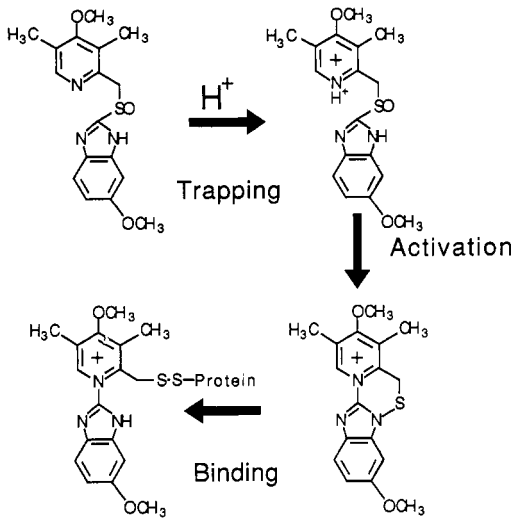

FIGURE 1: Reaction mechanism of omeprazole. The protonation of the pyridine nitrogen, $pK_a = 4$, results in accumulation in acidic space of the acid transporting vesicles. This is followed by an acid-catalyzed conversion to a cationic sulfenamide. The sulfenamide then reacts with SH groups on the H^+,K^+-ATPase to form disulfides.

inhibitors that interact with these pumps. Ouabain, a partially K^+-competitive inhibitor, has been shown to bind in the region of the first pair of membrane-spanning segments of the Na^+,K^+-ATPase (Price & Lingrel, 1988). The imidazo[1,2-*a*]pyridine Sch 28080[1] is K^+-competitive for the H^+,K^+-ATPase (Wallmark et al., 1987; Kaminski et al., 1985), and a photoaffinity analog of this compound, MeDAZIP$^+$, has been shown to bind to the extracytoplasmic loop in the M1/M2 region of the H^+,K^+-ATPase (Munson et al., 1991).

Omeprazole, a derivative (Figure 1) of 2-[[(2-pyridinyl)-methyl]sulfinyl]benzimidazole, is a covalent inhibitor of the H^+,K^+-ATPase in vivo and in vitro. It has a pK_a of 4 and is therefore concentrated in acid-transporting cytoplasmic-side-out vesicles of the H^+,K^+-ATPase isolated from hog gastric mucosa due to proton gradient dependent accumulation. In acid solutions, this compound undergoes an acid-catalyzed conversion to a cationic sulfenamide with low membrane permeability due to its permanent positive charge (Lindberg et al., 1986). Sulfenamides are able to react rapidly with free cysteines to form a disulfide. The sulfenamide of omeprazole is unable to react with disulfides. The chemical properties of this compound therefore make it selective for cysteines of the H^+,K^+-ATPase that are present in, or accessible from, the extracytoplasmic surface of the enzyme under acid-transporting conditions. Hence, in contrast to most group-selective regents (Pedemonte & Kaplan, 1990), this compound reacts in a sided manner with cysteines of the H^+,K^+-ATPase. Omeprazole inhibits the H^+,K^+-ATPase under these acid-transporting conditions with a stoichiometry of about 2 mol/mol of phosphoenzyme (Lorentzon et al., 1987; Keeling et al., 1987). The compound is therefore able to probe catalytically significant, cysteine-containing regions of the extracytoplasmic domain of the gastric proton pump.

[1] Abbreviations: PVDF, poly(vinylidene difluoride); Sch 28080, 3-(cyanomethyl)-2-methyl-8-(phenylmethoxy)imidazo[1,2-*a*]pyridine; MeDAZIP, 2,3-dimethyl-8-[(4-azidophenyl)methoxy]imidazo[1,2-*a*]pyridine; Tris, tris(hydroxymethyl)aminomethane; F-MI, fluorescein 5-maleimide; SDS, sodium dodecyl sulfate; CHAPS, 3-[(3-cholamidopropyl)-dimethylammonio]-1-propanesulfonate; Tricine, *N*-[2-hydroxy-1,1-bis(hydroxymethyl)ethyl]glycine; MDPQ, 1-(2-methylphenyl)-4-methylamino-6-methyl-2,3-dihydropyrrolo[3,2-*c*]quinoline; NEM, *N*-ethylmaleimide.

To determine which of the 28 cysteines of the α subunit and which of the nine cysteines of the β subunit were modified by omeprazole, the ATPase was labeled with either ^3H- (pyridine ring) or ^{14}C-(benzimidazole moiety) omeprazole under acid-transporting conditions. Tryptic fragments were generated from these labeled, intact vesicles and sequenced to determine the cysteines that had reacted with the labeled omeprazole. V8 protease digestion of the α subunit was necessary to define further the position of one of the labeled cysteines. From these data, it is shown that cysteines of the α subunit at positions 813 and/or 822 and the cysteine at position 892 were labeled. These are predicted to be in or between the fifth and sixth and between the seventh and eighth membrane-spanning sequences (M5/M6 and M7/M8) of the catalytic subunit, respectively, numbering the membrane sequences as for the Ca^{2+}-ATPase of sarcoplasmic reticulum (MacLennan et al., 1985). The absence of omeprazole labeling of the β subunit is evidence that the six cysteines in the predicted extracytoplasmic domain of this subunit are disulfide-linked.

MATERIALS AND METHODS

Preparation of Gastric Vesicles. Ion-tight vesicles were prepared essentially as described before (Sachs et al., 1976; Hall et al., 1991), which involved differential centrifugation to prepare a microsomal fraction as free as possible from mitochondrial contamination. This was followed by zonal density gradient centrifugation on a ficoll/sucrose gradient to remove residual mitochondrial fragments and to separate leaky from ion-tight vesicles. The fraction used for these studies on average showed a greater than 10-fold stimulation of ATPase activity in the presence of KCl with the addition of nigericin. Since the sided reaction of omeprazole requires acid gradient formation, it was essential to use preparations such as these that were ion-tight.

ATP Activity and Omeprazole Inhibition: (A) ATPase Activity. Basal ATPase activity is defined here as the Mg^{2+}-ATPase activity in the presence of 10 mM Hepes/Tris, pH 7.4. K^+-stimulated activity (20 mM KCl or K_2SO_4) in the absence of ionophores is due to leaky vesicles. The ATPase activity in the presence of nigericin in addition to 20 mM KCl or in the presence of 100 mM NH_4Cl was considered to reflect the total ATPase activity (Lorentzon et al., 1987), whereas the difference between the latter measurements and the K^+-stimulated ATPase reflects the fraction of ion-tight vesicles. The average basal activity in the experiments described here was 5 μmol of ATP hydrolyzed (mg of protein)$^{-1}$ h^{-1}; 10 μmol of ATP was hydrolyzed (mg of protein)$^{-1}$ h^{-1} in the presence of 20 mM KCl and 120 μmol (mg of protein)$^{-1}$ in the presence of KCl and nigericin. Accordingly, 90% or more of the ATPase activity in the vesicles required lumenal K^+ or the K^+ surrogate NH_4^+; i.e., 90% of the vesicles were ion-tight. NH_4^+ activates the ATPase by permeating as NH_3 and then forming NH_4^+, which is then transported by the H^+,K^+-ATPase out of the vesicles. NH_4^+ thus, while activating the pump, abolishes the H^+ ion gradient and prevents further omeprazole inhibition. P_i released was measured by the method of Yoda and Hokin (1970) and protein by the Lowry method (Lowry et al., 1951).

(B) Omeprazole Inhibition and Labeling of the ATPase. The principle used to determine the degree of omeprazole inhibition during labeling of the protein involved incubation with the chemical in a single reaction vessel with acid-transporting vesicles, removal of aliquots with time, stopping the omeprazole inhibition reaction by abolition of the pH gradient using NH_4^+, and determination of the residual NH_4^+-stimulated ATPase activity. This required determination of

the P_i released during the initial incubation and of the P_i released following termination of omeprazole inhibition.

The vesicles, at a concentration of 200 μg/mL, were added to a solution containing 250 mM sucrose, 125 mM KCl, 3 mM Tris, pH 6.9, and valinomycin at 1 μg/mL in the presence of 10 μM labeled omeprazole (specific activity 85–185 cpm/pmol). Duplicate 10-μL samples were removed at zero time for enzyme blank values, and MgATP was added to the main vessel at 5 mM final concentration to start the reaction at 37 °C.

Quadruplicate 10-μL samples were taken immediately after ATP addition and at 5-min intervals thereafter until 30 min. One set of duplicates was used for measurement of P_i released during the inhibition reaction and another set of 2 × 10-μL samples for measurement of residual ATPase activity. These samples were added to assay medium at 37 °C, and ATP was added to start the reaction. ATPase activity was measured in a solution of 40 mM Tris/HCl, pH 7, 100 mM NH_4Cl, and 250 mM sucrose in the presence of 2 mM MgATP at 37 °C for 15 min. The residual ATPase activity at each successive time point was obtained from the additional P_i released in the second incubation (Lorentzon et al., 1987). Better than 90% inhibition of ATPase activity was achieved at the 30-min time point at which the vesicles were used to determine the site of inhibition.

At 30 min, after the assay samples had been removed, the remaining reaction mixture was diluted 5-fold in ice-cold solution containing 250 mM sucrose, 15 mM KCl, and 20 mM Tris/HCl, pH 7. The mixture, after sitting for 2 h at room temperature, was spun in a Ti35 rotor for 1 h at 100000*g* and washed twice with 20 mM Tris/HCl, pH 7.0, and 250 mM sucrose before resuspension to a final protein concentration of 2–3 mg/mL in 20 mM Tris buffer, pH 7.4, and 250 mM reagent-grade sucrose. With the second wash less than 10% of the counts were removed from the labeled protein. The quantity of covalent label was obtained from counting 10 μL of the final suspension before and after precipitation with 10% TCA. A total of 65–85% of the counts remained with the TCA pellet. The average stoichiometry of labeling was 2.2 ± 0.3 (n = 9, ±SEM) nmol (mg of protein)$^{-1}$ in the preparations used.

(*C*) *Reversal of Labeling.* The addition of 10 mM mercaptoethanol removed all the acid-precipitable counts from the protein. From the chemistry of omeprazole it can be concluded that all the protein-incorporated counts are present in a disulfide linkage (Wallmark et al., 1985).

Tryptic Hydrolysis: (*A*) *Digestion at 1/40 Ratio in the Presence of Ligands.* The labeled H^+,K^+-ATPase (ca. 2 mg/mL) was treated with Sigma Type XIII trypsin (17 700 units/mg) at a trypsin to protein ratio of 1/40. The incubation was carried out at 37 °C for 10, 30, or 45 min in the presence of 250 mM sucrose, 50 mM Tris/HCl, pH 6.8, 0.2 mM Na_2-ATP, 25 μM Sch 28080, and 1 mM EGTA. The reaction was stopped by the addition of trypsin inhibitor (8-fold excess over trypsin). The membranes were centrifuged and resuspended to their initial volume and dissolved in sample buffer for electrophoresis as detailed below. The absence of iodoacetamide or NEM addition prior to digestion probably accounts for the lower yield of bound omeprazole with this procedure.

(*B*) *Digestion at 1/75 Ratio in the Absence of Ligands.* The labeled ATPase (ca. 2 mg/mL) was digested for increasing periods of time by trypsin as above, in the presence of either 100 mM iodoacetamide or 2 mM NEM but in the absence of ATP or Sch 28080, at a ratio of 1/75 trypsin to protein. The iodoacetamide or NEM was present in the digestion solution in order to improve the retention of labeled omeprazole following SDS solubilization and gel separation (Lorentzon et al., 1987). After digestion, further iodoacetamide (100 mM) was added and the membranes were freed of trypsin and soluble peptide fragments by centrifugation for 8 min in an airfuge at 20 psi. The membranes were then dissolved in 0.4% CHAPS in the continuing presence of iodoacetamide and delipidated by precipitation with 2 volumes of methanol on ice, and the pellet was dissolved in SDS as below. At each stage, a sample was teken to determine the distribution of counts either between membranes or supernatent or between methanol pellet and supernatant. A total of 66% of the radioactivity was retained in the methanol precipitate. HPLC separation showed that the radioactivity released into the supernatant was found to be converted drug no longer bound to peptide (see below).

(*C*) *Digestion at 1/4 Trypsin to Protein Ratio of Unlabeled or Labeled Enzyme and Treatment with Fluorescein 5-Maleimide.* The use of fluorescein maleimide subsequent to exhaustive digestion and washing was used for identification of retained pairs of membrane-spanning segments since each predicted pair has at least one cysteine. The labeled or unlabeled enzyme was digested with trypsin at an enzyme to protein ratio of 1/4 prior to FMI labeling.

Labeled or unlabeled intact vesicles (100 μg) were digested for 10 min under isotonic conditions as above, and the reaction was stopped by the addition of a 15-fold excess of trypsin inhibitor on ice. The membranes were washed by centrifugation at 100000*g* for 60 min. A total of 71% of the counts remained with the pellet under these conditions. The pellet was suspended in 100 μL of a solution containing 0.5% SDS, 50 mM Tris/HCl, pH 6.1, and fluorescein maleimide added at 50 μM final concentration to label the membrane-retained cysteines. Incubation was continued for 30 min at room temperature, and the solution was then added to 20 μL of electrophoresis sample buffer. The samples were electrophoresed on Tricine gradient gels and transferred to PVDF membranes as described below. The location of the F-MI-labeled bands was defined by the fluorescence of the PVDF membrane and the counts in the labeled enzyme located by slicing the membrane and counting as described. In one experiment the gel was sliced and its counts were compared to the counts transferred to the PVDF membrane. Counts at the dye front of the gel accounted for about 30% of the total counts but were not retained by the PVDF. In the experiment presented, ^{14}C-omeprazole was used to determine whether the instability of counts was a function of the site of tritiation (pyridine ring) as compared to the benzimidazole ring. The loss of counts after digestion and transfer was similar for the two sites of labeling.

V8 Protease Digest. As before (Munson et al., 1991) FPLC was used to separate the labeled α and the β subunits in the solubilized enzyme, and then the labeled α subunit was digested, followed by SDS gel separation and sequencing. Labeled protein (3 mg) was dissolved in 2% SDS and loaded on a FPLC Superose-6 column. The α subunit was eluted with 50 mM Tris/HCl, pH 7.8, and 0.05% SDS at 0.2 mL/min and concentrated in a speed vacuum lyophilizer. The subunit (600 μg) was digested by 40 μg of V8 protease at 37 °C for 4 h, methanol was added (2 volumes), and the suspension was precipitated by centrifugation. The pellet was resuspended in 200 μL of 20 mM Tris, pH 7, solubilized in electrophoresis sample buffer, and separated on a Tricine gradient gel as before. A 7.5-kDa labeled peptide was identified as the

smallest radioactive fragment by autoradiography and counting. This was sequenced as detailed below.

HPLC Separation of Supernatant Radioactivity. The supernatant from a trypsin digest was concentrated by lyophilization and injected onto a C18 column using a Beckman HPLC system, with linear gradient elution using 0.1% TFA and 80% acetonitrile/20% 2-propanol as the two solvents. The counts eluted with a retention time of 19 min. Acid-converted omeprazole eluted with exactly the same retention time, indicating that the supernatant counts were reaction products eliminated from the protein during the preparation of the digest.

SDS Gel Separation. The suspended membranes or methanol precipitate of the membrane residue were combined with 20% volume of sample buffer (0.3 M Tris, 10% SDS, 30% sucrose, and 0.025% bromphenol blue), and the solution was placed on top of a 10% (34:1 acrylamide/methylenebis-[acrylamide]) to 21% (17:1 acrylamide/methylene bis-[acrylamide]) 1.5-mm gradient slab gel using the Tricine buffer method (Schagger & von Jagow, 1987). The gel was run in the cold room (4 °C) for 18 h at 90 V constant voltage, along with a lane for prestained MW (Sigma 106–18 kDa) standards and CNBr fragments of horse myoglobin (Sigma, 17–2.5 kDa). In every case a duplicate lane was run, to provide sufficient material for sequencing. Reducing agents were absent in all experiments since these displace the bound omeprazole.

Standard curves of ln MW as a function of relative mobility were used to estimate the MW of the peptide products of digestion. The accuracy of the MW determination appeared to be within 10% based on predicted tryptic cleavage sites within the primary sequence of catalytic subunit of the enzyme.

The peptides were transferred electrophoretically to PVDF membranes (Millipore) for 18–24 h in the cold room (4 °C) in a tank transfer apparatus at 120 mA constant current in a transfer buffer of 0.15 M glycine, 0.02 M Tris, and 20% methanol. A sandwich of three sheets of Whatman 3MM filter paper was placed on either side of the gel, which had a prewetted PVDF membrane on the anode side. After transfer, the blots were rinsed twice in distilled water and stained with Coomassie blue in 10% glacial acetic acid and 45% methanol.

Identification of Radioactive Bands. One-third of one lane of the PVDF membrane was sliced into 1-mm sections, and the pieces were dissolved in dimethylformamide and counted in liquid scintillant in a LKB scintillation counter. Alternatively, the PVDF membrane was sprayed with Enhance (NEN), placed on X-ray film, and exposed for 10–14 days at −80 °C. The position of the radioactive bands was identified by pin holes made through the X-ray film overlaid on the PVDF membrane. The bands identified as radioactive by either method were cut out from the PVDF membrane and sequenced. On occasion, nonradioative peptide bands were also sequenced to determine the general regions of labeling. The N-terminal end thus was established by direct sequencing. The C-terminal end was identified by MW of the band and the presence of arginine or lysine residues which would terminate the band to give a size close to the measured MW. The possibility exists that there is anomalous migration of bands to give an erroneous MW, but the calculated and measured values corresponded very well. Nevertheless, although it is convenient to refer to the beginning and end position of a given peptide, in some instances these may be outside the 10% error limit we have assumed throughout.

Sequencing. Both radioactive and nonradioactive bands were sequenced with a gas-phase sequencer at the UCLA Protein Microsequencing facility using the Applied Biosystems 475A system composed of a 470A sequencer, a 120A phenylhydantoin analyzer, and a 900A data module.

To identify the presence of a given sequence, each amino acid position was inspected for elevation at a particular cycle and decrease at a subsequent cycle. The quantity of a given peptide was obtained by averaging the elevation above background for the amino acid in each cycle for sequencing cycles 2–7. In most instances the sequence could be followed for 10 cycles. With 80–100 μg of protein loaded per lane of the gel, it was often necessary to sequence bands from two duplicate PVDF lanes to have sufficient quantities of peptide for clear sequence identification (Munson et al., 1991).

Stoichiometry of Peptide Labeling. The counts in the 1-mm PVDF slice allowed calculation of the amount of omeprazole bound as compared to the amount of sequence found in the analyzer. Typically about a third of the applied counts were recovered on the PVDF membrane following electrotransfer. About 30% of the counts were found at the bottom of the gel and these were not retained on the PVDF membrane, showing that there had been progressive loss of label from peptide.

Materials. The materials used were of the highest grade of purity available. Trypsin was obtained from Sigma; PVDF membranes were from Millipore. ^{3}H- or ^{14}C-omeprazole was a gift from Astra-Hassle AB, Molndahl, Sweden. Fluorescein 5-maleimide was obtained from Molecular Probes.

RESULTS

Hypothetically, 97 fragments would be produced by full trypsinization of the α subunit of the enzyme. The use of intact vesicles reduces this number somewhat since extracytoplasmic cleavage sites are protected. Intact vesicles also prevent hydrolysis of the large extracytoplasmic domain of the β subunit. In the case of the digest in the presence of Sch 28080 and ATP, only two major fragments are produced, allowing the general region of labeling to be determined. In the 1/75 trypsin to protein ratio digest, several fragments are produced, whereas in the 1/4 digest, fewer fragments are found which represent the retained membrane-embedded segment pairs. When data from these digests are combined with the V8 protease digest results, the sites of omeprazole labeling can be determined.

Presentation of Data. The data for each tryptic digest are summarized schematically in the figures describing the tryptic digestion. Here all the sequences obtained in a given band are shown, along with the MW, the yield of peptide, and the recovery of omeprazole in the radioactive bands. The sites of tryptic cleavage detected by the peptides sequenced in a particular experiment are shown in relation to the eight membrane-spanning segments detected in the 1/4 trypsin to protein digestion experiment. In discussing the amino acid sequences identified, the numbering is based on the known N-terminal amino acid sequence and hence is one less than the cDNA-derived sequence (Lane et al., 1986). In each figure the deduced positions of the reacted cysteines are shown to clarify the relationship between sequence and radioactivity. The data are presented as a function of increasing cleavage of the enzyme, along with the labeling results.

Trypsin Digestion of Unlabeled Enzyme at a 1/4 Trypsin to Protein Ratio. This method was used, followed by labeling with F-MI, to produce and detect the membrane-spanning segments of the catalytic subunit of the gastric H^+,K^+-ATPase. This protocol cleaved the enzyme rapidly and virtually completely on the cytoplasmic face. Cleavage, while remaining sided, would be as close as structurally possible to the

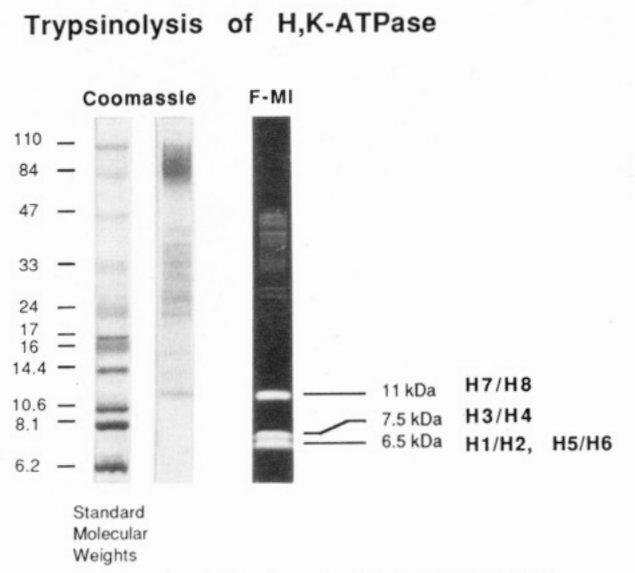

FIGURE 2: Results of digestion of unlabeled H+,K+-ATPase at a trypsin to protein ratio of 1/4. On the left is a MW standard lane; in the middle, Coomassie staining of the digested membranes following SDS solubilization and reaction with F-MI; and on the right, the fluorescent pattern, showing the lower MW fluorescent peptides that were sequenced. Beside these are illustrated the hydrophobic regions that these peptides represent.

membrane-embedded segments of the enzyme and should leave a segment pair joined by an extracytoplasmic loop in the membrane. Each of these as predicted by hydropathy has at least one cysteine. This allows labeling of the retained membrane-associated SH groups by fluorescein maleimide and sensitive detection of the fragments.

Figure 2 shows that three fluorescent bands were detected, at 11.2, 7.5, and 6.5 kDa. Only the 11.2-kDa band can be detected by Coomassie staining. The 11.2-kDa band contained a unique sequence, beginning at Leu^{853} and predicted to extend to Arg^{946}. This would derive from M7 and M8. The second band, of 7.5 kDa, also had only one sequence, beginning at Thr^{291} and probably reaching Lys^{358}. This would contain M3 and M4. The 6.5-kDa band contained two sequences: one began at Gln^{104} and was inferred to extend to Lys^{162}, and the other began at Leu^{776} and would be predicted to end at Lys^{835}. The first of these would correspond to M1 and M2 and the second to M5 and M6.

The absence of a fluorescent band corresponding to H9/H10 as predicted by hydropathy is unexpected, since there are four cysteines present on H9. It is possible that this region is membrane-embedded and not membrane-spanning and hence is relased following cleavage and washing. It is also possible that these cysteines are disulfide-linked, but this would imply either cross-linking with other intramembranal cysteines or a nonhelical structure. Reduction with dithiothreitol prior to F-MI labeling did not result in a band corresponding to H9 or H10, but the band corresponding to the region of the β subunit became fluorescent (data not shown). Given the absence of data proving the presence of M9/M10 in this or any other digest, this membrane pair has been omitted from the model proposed, since the model is based only on the data obtained in this work. Hence the region is shown as membrane-associated rather than membrane-spanning in the model illustrated in the schematics and in Figure 7.

Trypsin Digestion of Labeled Enzyme in the Presence of ATP and Sch 28080. We have shown previously that tryptic digestion in the presence of Sch 29080 and ATP results in very limited cleavage of the α subunit (Munson et al., 1991)

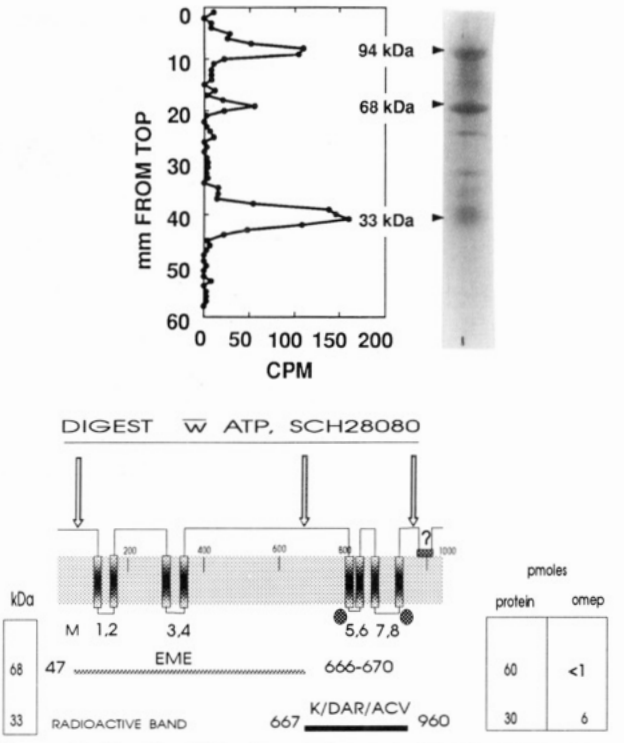

FIGURE 3: Results of digestion of the labeled H+,K+-ATPase in the presence of ATP and Sch 28080. (Top) The count profile obtained by slicing the gel is on the left, and the Coomassie staining is on the right. The bands sequenced are indicated by arrows. (Bottom) Schematic diagram of the results of this digest, showing the MW of the peptides found and sequenced, as well as their quantity on the PVDF membrane along with the determined amount of omeprazole bound to the protein fragments. The N-terminal amino acids are immediately above the diagrammed peptide fragment; to the right is shown the position of the N-terminal fragment, and to the left the calculated (based on MW and the presence of Lys or Arg) C-terminal position. It should be noted that the eight-membrane-segment model shown at the top of the panel corresponds to the data obtained here and contains the first eight segments of the 10 membrane-spanning segment model of the Ca^{2+}-ATPase. The arrows indicate the main tryptic cleavage sites. This schematic is repeated for all the digest diagrams. The cysteines labeled are indicated by circles.

compared to that in the absence of these ligands, because of the conformation of the stabilized E_2P form of the enzyme. The same pattern was found with omeprazole-labeled enzyme. Both ATP and Sch 28080 were required to give the restricted cleavage pattern described below. The conformational effect of these ligands indicates that ATP and Sch 28080 bind to the enzyme even after omeprazole has reacted with the protein.

Two major peptides were produced in high yield at this trypsin to protein ratio of 1/40 at 30 min as defined either by Coomassie staining or by yield of sequence (Figure 3). The same pattern was seen at 10 min and persisted even at 45 min.

The larger peptide of about 68 kDa had as its N-terminal sequence EME, which begins at position 47 in the α subunit chain and should extend to about position 670 in the linear sequence of the α subunit based on MW. Since the smaller fragment begins mainly at position 671, the likely termination of the major 68-kDa fragment is at Arg^{670} (Figure 3, bottom).

Sixty picomoles of this fragment was detected in the experiment presented when 160 μg of digested enzyme protein was placed on the gel. Since this cleavage at Lys^{46} and at Arg^{670} occurred rapidly in the inside-out enzyme, these are likely to be cytosolic sites, placing the N-terminus of the α subunit on the cytoplasmic side of the membrane.

The smaller of the two peptides had a mass of 33 kDa and the N-terminal sequences were ACV (major), DARACV,

and KDARACV, beginning at positions 671, 668, and 667, respectively, in the linear sequence of the enzyme. Thirty picomoles of these sequences was recovered from 160 μg of protein in this particular experiment. From the MW of the fragment and lysine or arginine positions, the C-terminal end of this fragment would be expected to be at about position Arg^{960}; hence this site is also likely to be cytoplasmic. The cutting site at the end of this fragment would be expected to be just ahead of the last hydrophobic region of the enzyme. In three experiments where sequence was determined, the average yield was a total of 33 pmol for these sequences, about half of the yield of the larger fragment.

In terms of omeprazole labelling, the larger fragment had little or even no associated radioactivity. In six experiments, 15% of the counts were found in the 68-kDa peak as compared to 85% in the 33-kDa peak. There was also no radioactivity found below the 33-kDa band on the PVDF membrane, which could contain the C-terminal fragments beyond about position 960. The cysteines that react with omeprazole are therefore mainly in the region of the enzyme between positions 667 and 960.

These results are presented schematically in Figure 3 (bottom). The three tryptic cleavage sites revealed by sequencing conform to the cytoplasmic location of these sites as postulated by the model illustrated.

Trypsin Digestion of Labeled Enzyme in the Absence of Ligands. The ligand digest showed that the major labeling by omeprazole was in the C-terminal third of the protein between positions 667 and 960. In the ligand-free digest, where the fragmentation pattern was more complicated, peptides containing cysteines within this region of the enzyme were potentially labeled. Peptides from outside this area were assumed not to contribute to the radioactivity.

Trypsin Digestion of Labeled Enzyme at a 1/75 Trypsin to Protein Ratio. When intact vesicles were incubated for 5 min or longer with trypsin at a trypsin to protein ratio of 1/75, a relatively complicated peptide and radioactivity profile was obtained as shown in Figure 4 (top). In this panel, the Coomassie pattern, radioactive profile, and autoradiographic pattern are shown.

There were three major peaks of radioactivity identified by slicing the gel, associated with peptide peaks below the unhydrolyzed α subunit, at 40, 24.5, and 10 kDa, with some smearing of radioactivity toward the top of the gel and below the 40-kDa peak. Autoradiography of the gel showed these same bands but allowed additional identification of other bands, for example at 14 and 18 kDa. Various radioactive bands at or below 40 kDa were sequenced from this gel to further identify the omeprazole site. Some nonradioactive bands were also sequenced so as to compare the general region of retained label with that found with digestion in the presence of ATP and Sch 28080. The results are summarized in Figure 4 (bottom).

Unlabeled Bands. Two major bands showing Coomassie staining at 78 and 72 kDa were devoid of radioactivity. For both the only detected sequence began at position number 47 (EME), and these peptides can be inferred to extend to Lys^{752} and probably Lys^{707}, respectively, to give the determined MWs. This confirmed that the results of the digest in the presence of ATP and Sch 28080 were not due to selective removal of omeprazole by these ligands and that the N-terminal $^2/_3$ of the enzyme bound little omeprazole. Further, it can be predicted that the cysteines reacting with omeprazole must be subsequent to Lys^{752}. The yield of these two sequences from 160 μg of protein was 6 pmol.

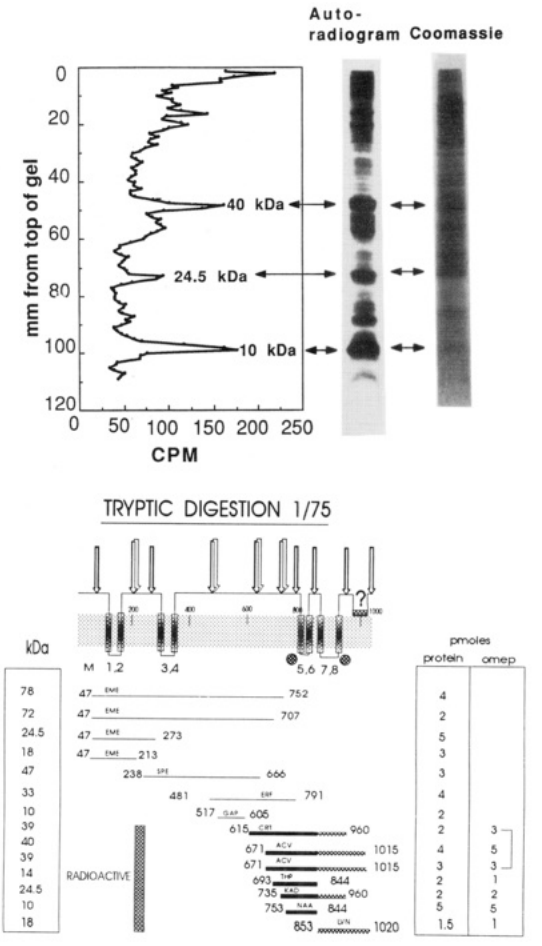

FIGURE 4: Results of digestion of the labeled H^+,K^+-ATPase in the absence of ligands at a trypsin to protein ratio of 1/75. (Top) This panel displays on the left the count profile, in the middle the autoradiogram, and on the right the Coomassie staining. The bands sequenced are indicated by arrows. (Bottom) Schematic diagram of the results of this digest, showing the various parameters that were determined, namely, sequence and quantity of sequence at the specified MW and amount of omeprazole found on the PVDF membrane at the locations indicated. Again the N-terminal amino acids are indicated on top of the peptide fragment, with the N-terminal position to the right and the C-terminal position to the left. The diagram of the membrane-spanning peptides on the top represents the segments demonstrated here. The arrows point to the sites of tryptic cleavage found as determined by sequencing many of the membrane-retained peptides. The cysteines labeled are indicated by circles.

Two other nonradioactive bands were sequenced, one of 47 kDa beginning at position 238, SPE, which would be predicted to extend to about Arg^{666}, and another of 33 kDa beginning at 481, ERF, probably extending to Lys^{791}. The first of these would contain predicted membrane-spanning sequences M3 and M4 and would be expected to be retained after washing of the digested membranes. The second is not predicted to be membrane-inserted but might be membrane-associated and hence be partially retained during the washing procedure. The finding that this band is devoid of radioactivity places the labeled cysteines probably subsequent to position 791.

Labeled Sequences. When the radioactive 40-kDa band was sequenced, this began at position 671 (ACV), probably extending to position Arg^{1015}. Sequence from 1 mm below this band (39 kDa) showed the same sequence with an additional sequence beginning at position 615, CRT, which would be predicted to extend to Arg^{960}.

The band at 24.5 kDa, in addition to a sequence containing M1 and M2, had a sequence beginning at Lys^{735} which would extend to Arg^{960} from its MW. From the limited digest

discussed above, this would be predicted to contain bound omeprazole. This sequence contains seven cysteines that could react with omeprazole.

The 18-kDa band also contained, in addition to the EME sequence beginning at position 47, a sequence beginning at LVN at position 853. The sequence analysis and MW predict that this sequence would extend from Leu[853] to Arg[1020]. This fragment contains Cys[892] as well as two other cysteines prior to Arg[960].

The sequences at 24.5 and 18 kDa also contained the EME sequence beginning at position 47. Both peptides would contain the first pair of membrane-spanning segments but not the second pair as predicted from hydropathy analysis. These peptides are therefore produced by cleavage on either side of the first membrane pair, and these cleavage positions would be expected to be cytosolic. Retention of these fragments is presumably dependent on the presence of membrane-inserted regions. Since these are known to be nonradioactive from the ligand digest results, these peptides did not account for the counts found at this location on the PVDF membrane.

The 14-kDa radiolabeled sequence began at position 693 (THP) and from MW would extend to about Arg[844]. This band would contain cysteines 813 and 822, as would the 40- and 39-kDa bands described above.

When the 10-kDa radioactive band was sequenced, it yielded a sequence beginning at position 752 (NAA), which from MW and tryptic sites would also extend to about Arg[844]. Only two cysteines are contained within this region, those at positions 813 and 822. The amount of sequence found was 5 pmol. Labeling of one or both of these cysteines is consistent with sequence and radioactivity profiles obtained from both this and the former digestion protocol.

There was a sequence at the 10-kDa region beginning at position 517, GAP, just subsequent to the Lys[516] that reacts with FITC. From MW this sequence would extend to Arg[605], and retention of this sequence after digestion and washing is unexpected. However, it would not contain labeled omeprazole.

The above data show that one of the two sites labeled by omeprazole is at either Cys[813] and/or Cys[822]. Another cysteine between Cys[822] and Arg[960] is also labeled as shown by the radioactivity in the 24.5- and 18-kDa bands.

The positions of the tryptic cleavage sites relevant to secondary structure of the α subunit are shown in Figure 4 (bottom). There are many more than in the digest in the presence of ligands. All of the sites detected conform to the eight-membrane-segment model illustrated.

The radioactive sequences are illustrated at the bottom of the panel, in thicker solid or hatched lines. Adding the total yield of these sequences and comparing this to the total recovery of omeprazole in these regions gives a stoichiometry close to 1.

The β subunit remained largely intact, suggesting a mainly extracytoplasmic location for this subunit. Because of the glycosylation of this subunit resulting in broadening of the band, it is difficult to detect N-terminal cleavage prior to the postulated membrane-spanning sequence. It is clear, however, that little if any of this subunit is cleaved under intact vesicle conditions, in contrast to solubilized enzyme (Munson et al., 1991).

Digestion of Labeled Enzyme at a 1/4 Trypsin to Protein Ratio. Figure 5 (top) (typical of four experiments) shows Coomassie staining, fluorescence, and radioactivity. There were three bands of fluoroescence detected at 11.2, 7.5, and

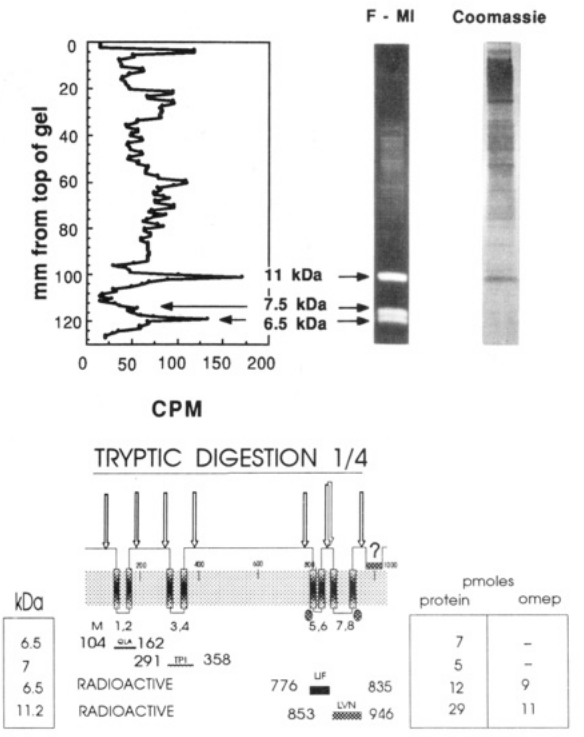

FIGURE 5: Results of digestion of the labeled H+,K+-ATPase at a trypsin to protein ratio of 1/4, followed by labeling with F-MI as detailed in the text. (Top) The fluorescence and Coomassie staining are displayed along with the count profile of the sliced PVDF membrane. Only the 11.2-kDa band had Coomassie staining. (Bottom) Schematic diagram summarizing the results of this experiment, displaying the MW, amount of sequence, and amount of associated omeprazole, along with the position of the membrane pairs determined by sequencing the fluorescent bands, with repect to the eight-membrane-segment model. The cysteines labeled are indicated by circles.

6.5 kDa, as for unlabeled enzyme. The highest MW band had again a unique sequence beginning at Leu[853]. This sequence would encompass membrane segments 7 and 8 and was radioactive. The second band again had only one sequence beginning at Thr[291]. Few counts were found at this position. The smallest band had, as for unlabeled enzyme, two sequences, one beginning at Gln[104] and the other beginning at Leu[776]. The former would correspond to membrane segments 1 and 2 and the latter to segments 5 and 6 in the new eight-membrane-segment model. This band was also radioactive, accounted for by the presence of M5/M6. M1/M2 labeling has already been excluded by the more limited tryptic digestion results.

Since radioactivity was found only in the 11- and 6.5-kDa bands, this would correspond to the two labeling regions deduced previously. The 11-kDa band contains Cys[892], Cys[927], and Cys[938], whereas the 6.5-kDa band contains Cys[813] and Cys[822]. The sequence beginning at Gln[104] has already been excluded as a significant labeling site for omeprazole, on the basis of the digest in the presence of ATP and Sch 28080 above (Figure 3) and the digest at 1/75 trypsin to protein ratio (Figure 4). It should be noted that the sequence containing membrane segments 3 and 4 had very little radioactivity, although Cys[321] has been suggested to be the omeprazole site (Morii et al., 1990) as discussed below. These data are presented in the schematic of Figure 4 (bottom). The radioactive sequences are presented in thicker black or hatched lines. The stoichiometry of the M5/M6 labeling was 0.8, whereas in the M7/M8 region it was about 0.3.

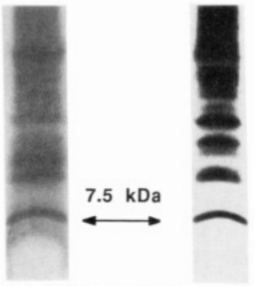

FIGURE 6: Results of digestion of the labeled α subunit of the H^+,K^+-ATPase with V8 protease. The autoradiogram of the 7.5-kDa sequenced region is displayed alongside the Coomassie-stained lane.

Since $Cys^{813/822}$ and $Cys^{892/927/938}$ should be extracytoplasmic, either there is a pair of membrane segments between these residues or these cysteines are contained within a single large extracytoplasmic loop. Cleavage by trypsin in the region between 844 and 852 argues that this sector is exposed on the cytoplasmic face of the enzyme. Hence the positions of the labeled cysteines coupled with the tryptic hydrolysis pattern show that there is a pair of membrane segments between the cysteines at position 822 and 892 or 927/938.

Protease V8 Digest. The tryptic digest data gave evidence for labeling of either cysteine 813 or 822 and another cysteine subsequent to these. From sequence data, the likely cysteines subsequent to Leu^{853} were at position 892, 927, or 938. As with MeDAZIP$^+$ studies, V8 protease digestion was used to provide an alternative cleavage method, since it had been shown that a single peptide containing Cys^{892} was produced at 7.5 kDa when the unmodified solubilized catalytic subunit of the enzyme was digested with this protease (Bamberg et al., 1992).

Analysis of the protease V8 digest at the 7.5-kDa region (Figure 6), where labeling was detected by autoradiography, demonstrated the presence of only a single sequence, beginning at Ser^{838} as described previously (Bamberg et al., 1992). Based on MW, this fragment extends to about Glu^{900}. These data show that Cys^{892} is labeled, since there is no other cysteine in this sector of the enzyme. Hence the combination of tryptic and V8 protease digestion has shown that the sites of labeling are at Cys 813 or 822 and at Cys 892.

Stoichiometry of Peptide Labeling. The initial stoichiometry in nine experiments was 2.2 nmol (mg of protein)$^{-1}$. Following digestion in the presence of ATP and Sch 28080, the recovery of omeprazole was 6 pmol in the band containing 30 pmol of the labeled peptide. Since no other α-subunit-derived peptide was found, the stoichiometry of omeprazole labelling is about 0.2 in this band. This recovery was significantly lower than that found in the absence of ligands.

In the 1/75 trypsin/protein experiments, recovery of omeprazole in all the radioactive bands was 17 pmol, compared to a total peptide fragment content also of 17 pmol, as illustrated in Figure 4. This gave an overall stoichiometry of 1. The 1/4 digest recovered 20 of pmol omeprazole as compared to 41 pmol of the radioactive sequences (Figure 5). The 1/75 digest was performed using ^{3}H-omeprazole labeled in the pyridine ring, whereas the 1/4 digest used ^{14}C-omeprazole labeled in the benzimidazole moiety. The similar count recovery suggested that loss of counts was due to loss of the whole molecule and not due to the elimination of just part of the bound compound.

The stoichiometry of omeprazole as compared to the peptide(s) containing Cys^{813} or Cys^{822} was close to 1:1. For example in the 1/4 digest the omeprazole recovery showed a stoichiometry of 0.8 with respect to the M5/M6 peptide, as compared to 0.4 for the M7/M8 peptide containing Cys^{892}.

Overall, the recovery on the PVDF membrane in terms of added counts was 30%. When the acrylamide gels run in parallel were sliced, 30% of the counts were at the dye front, which were not transferred to PVDF and probably resulted from breakdown of the labeled fragments. Hence it is likely that the initial stoichiometry for the peptide fragments was at least 2-fold greater than that determined for the separated bands.

DISCUSSION

Topology of the α Subunit. In principle, topological information should be obtained from the tryptic cleavage pattern of these intact, inside-out vesicles. The assumption that trypsin does not penetrate the vesicle membrane with short incubation times seems reasonable. Direct evidence was obtained in the 1/4 tryptic digest, where it was shown that larger peptides labeled by F-MI were not cleaved unless NP40 was added prior to digestion (data not shown). Further, trypsin-sensitive sites in the extracytoplasmic loop between M7 and M8 were not cleaved and the β subunit remained intact.

The cleavage of the H^+,K^+-ATPase by trypsin in intact inside-out vesicles is different in the presence and absence of ligands, showing that the trypsin-sensitive bonds have very different accessibility depending on enzyme conformation. In the conformation induced by ATP and Sch 28080, out of a total of 39 lysines and 52 arginines beyond Lys^{46}, only six were observed to be cleaved (Lys^{46}, Arg^{666}, Lys^{667}, Arg^{670}, Arg^{960}, and Arg^{1015}). In the C-terminal third of the enzyme, where the omeprazole labeling is located, there are 12 lysines and 18 arginines. Of these 30 possible cleavage sites, only three appear to be hydrolyzed when the enzyme is in the ATP·E_2·Sch 28080 conformation. This implies a lack of accessibility of trypsin to most of the scissile bonds of the positively charged amino acids of the α subunit in this conformation.

When the protein is analyzed by an algorithm predicting the radial or buried location of tryptic cleavage sites (Nishikawa & Oi, 1986), all of the observed cleavage sites in the ligand-protected form are calculated to be radial, in particular the sites at Lys^{46}, Lys^{667}, Arg^{960}, and Arg^{1015}.

The initial sites of tryptic cleavage in the presence of ligands show that the N- and C-terminal sectors are cytoplasmic, along with the sites around positions 670 and 960 and 1015. The cytoplasmic location of the C-terminal sequence as derived from the tryptic cleavage map is consistent with results derived from iodination of the C-terminal tyrosines (Scott et al., 1992).

The use of fluorescein 5-maleimide to detect small cysteine-containing peptides, after the 1/4 trypsin/protein ratio cleavage of the enzyme in intact vesicles, provided convincing evidence for four pairs of membrane-embedded sequences corresponding to M1/M2, M3/M4, M5/M6, and M7/M8. As can be seen in Figures 2 and 5, this labeling technique also allowed clear identification of these four membrane segment pairs, in contrast to either Coomassie or silver staining. Thus this method confirmed the hydropathy prediction for the first four membrane-spanning segments but showed that the hydropathy analysis of the C-terminal third of the protein is inconsistent with experimental data, in particular by proving the presence of the M5 amd M6 membrane-spanning sequences between positions 776 and 835.

The hydrophobicity plot for the catalytic subunit of the H^+,K^+-ATPase is presented in Figure 7 along with the eight-

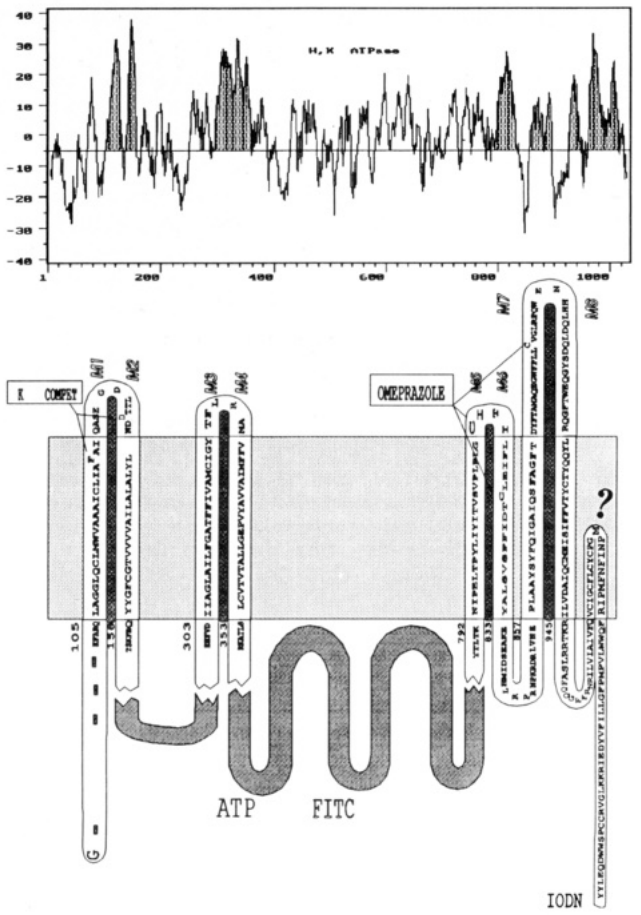

FIGURE 7: On top is the hydropathy profile of the catalytic subunit of the H+,K+-ATPase of hog analyzed by the Kyte–Doolittle algorithm using an 11 amino acid average. Below is aligned approximately a working model of the membrane arrangement of the H+,K+-ATPase α subunit. The sites of tryptic cleavage that were found determine the eight-membrane-segment model that is displayed. The putative beginning and ending positions of each pair are numbered. The cysteines shown to react with omeprazole are connected by lines to the omeprazole box. Also shown are the sites for K^+ competitive antagonist binding, the accessibility of cytoplasmic tyrosines to iodination in intact, cytoplasmic-out vesicles, and the ATP and FITC binding regions in the third intracellular segment. In view of the current lack of physical evidence for the arrangement of the putative M9 and M10 segments, these are displayed as membrane-embedded rather than membrane-spanning.

membrane-segment model determined biochemically for the H+,K+-ATPase. The last two hydrophobic sequences are depicted as membrane-embedded, rather than membrane-spanning, given the absence of F-MI-labeled peptides from this region in the 1/4 digest. Nevertheless, this work has not proved their absence from the membrane. Indeed, in vitro translation of the ninth hydrophobic sequence in pancreatic microsomes shows that this sequence can span the microsomal membrane (K. Bamberg and G. Sachs, unpublished observations).

In spite of an overall homology of only 15% between the H+,K+-ATPase of gastric mucosa and the Ca^{2+}-ATPase of sarcoplasmic reticulum, the hydropathy plot and suggested location of predicted membrane-spanning sequences are virtually identical (Maclennan et al., 1985; Matthews et al., 1990; Clark et al., 1989), suggesting a structural membrane motif for these two enzymes not evident from amino acid homology. The eight membrane segments derived from the hydrolysis data are thus superimposable on the model of the Ca^{2+}-ATPase, with the exception of the proposed sequences M9 and M10 in the Ca^{2+}-ATPase. The 10-membrane-segment model of the Ca^{2+}-ATPase of sarcoplasmic reticulum is based in part on results defining the sidedness of antibodies to the region 877–888, where ELISA reactions in intact and detergent-treated vesicles showed reaction only following detergent treatment of the membranes (Matthews et al., 1990; Clarke et al., 1990). Mutation studies which affected Ca^{2+} interaction with phosphoenzyme were guided by the 10-membrane-segment model and the results were consistent with the concept that critical hydrophilic sites were intramembranal (Clarke et al., 1989).

A 10-membrane-segment model has been discussed recently for the Na+,K+-ATPase based on sequences found using a variety of proteases such as proteinase K, trypsin, and pronase (Capasso et al., 1992), where the terminal 19-kDa fragment of the enzyme was relatively protease-resistant. This protease resistance was interpreted as evidence for a mainly membrane location of this sector. On the other hand it has been suggested that the H+-ATPase of *Neurospora* has 12 membrane-spanning segments (Subrahmanyeswara-Rao et al., 1991).

Alignment of these EP-type pumps has led to the suggestion that all of them have at least 10 membrane-spanning segments (Green, 1989). The membrane topology of the EP-type pumps is clearly an area of controversy, but it would seem likely that they all conform to the same pattern, be it 8, 10, or 12 membrane-spanning helices. The work here provides physical evidence for at least eight membrane-spanning segments of the α subunit of H+,K+-ATPase.

Topology of the β Subunit. The β subunit was not or was barely digested during trypsinolysis, which is consistent with the presumed orientation of the β subunit, with only about 40 amino acids present in the cytoplasmic domain. When detergent-treated vesicles were digested, it was a consistent finding that with reducing but not with nonreducing gels a fragment consisting of the last 45 amino acids beginning with the sequence AQP (position 241 in the cDNA sequence) was found to be generated (Munson et al., 1991). Hence this region of the β subunit is extracytoplasmic and the cysteines at positions 201 and 262 are disulfide-linked. The hydropathy plot is therefore probably correct in predicting a single membrane-spanning segment in the β subunit between positions 36 and 63.

Sites of Labeling: (*A*) *α Subunit.* The cleavage of the enzyme in the presence of ligands that stabilize the E_2P form of the enzyme produced two fragments, predicted to span residues 47–670 and 670–960. Most of the label was found in the latter fragment. Tryptic cleavage in the absence of ligands was performed at trypsin to protein ratios of 1/75 and 1/4. This resulted in the first instance in the production of several peptides that were sequenced. By excluding the peptide fragments in radioactive bands that originated prior to position 679, it was possible to conclude that the labeled cysteines were at position 813 or 822 and probably at position 892, 927, or 938. The results of the 1/4 tryptic digest also showed that the labeling was associated with membrane segment pairs with sequences spanning positions 776–835 and 853–946. These correspond to the M5/M6 and M7/M8 membrane segment pairs and their connecting extracytoplasmic loop. V8 protease digestion of the solubilized separated α subunit excluded labeling of cysteines 927 and 938 and led to the deduction that cysteine 892 was labeled. The labeling sites of this sided cysteine reagent therefore confirm the presence of the M6/M6 and M7/M8 segments as defined by tryptic hydrolysis.

Previous work (Morii et al., 1990) claimed that Cys^{321} was the omeprazole labeling site, proposed to be at the end of the

third membrane-spanning segment. However, these experiments used UV irradiation of omeprazole-reacted enzyme in order to produce a fluorescent derivative of the bound sulfenamide. Reaction with thiols such as glutathione did not result in fluorescence after UV irradiation, suggesting that the fluorescence was environment-specific. Hence, the method would not detect all the omeprazole sites. Perhaps the small amount of label we observed in the larger of the two fragments produced in the protected digest and the counts associated with M3/M4 corresponds to this site of labeling. Evidently, however, this is not the major site involved in the inhibition of the enzyme by omeprazole when radioactive omeprazole is used to determine the sites of labeling.

In contrast to omeprazole, inhibition by the K^+-competitive reagent Sch 28080 (Munson et al., 1991) is thought to be due to binding to Phe^{124} and Asp^{136}, located at the interface between fatty acid and phospholipid head groups in the M1/M2 region and the connecting extracytoplasmic loop. This region undergoes conformational change with phosphorylation (Rabon et al., 1991). It would therefore appear that inhibition of the H^+,K^+-ATPase by omeprazole may be due to the binding of the sulfenamide to the M5/M6 region of the enzyme since this is located also at the region of the phospholipid head groups. Binding of a bulky cation such as the sulfenamide in the M5/M6 region then inhibits phosphorylation (Wallmark et al., 1985) and binding of Sch 28080 to the M1/M2 region stabilizes the phosphoenzyme form (Keeling et al., 1989; Mendlein & Sachs, 1990).

Cys^{892} is in the loop between M7 and M8, which is projected to be in a relatively hydrophilic, large extracytoplasmic loop. Since the sulfenamide is formed inside the vesicles and is free to diffuse in the aqueous phase of the vesicles, reaction with this cysteine is likely chemically but may be unrelated to inhibition. Data to be published elsewhere show that pantoprazole, 2-[[(3,4-dimethoxy-2-pyridinyl)methyl]sulfinyl]-7-(difluoromethoxy)benzimidazole, a chemical congener of omeprazole, is equally effective in inhibiting the acid-transporting H^+,K^+-ATPase but labels only Cys^{813} and Cys^{822} (Shin et al., 1993). The greater stability of the protonated form of pantoprazole may allow binding of the protonated form of this compound to the enzyme prior to the formation of the sulfenamide, which will then be able to react in situ.

In experiments where H^+,K^+-ATPase fragments were adsorbed onto bilayers, it was found that omeprazole was able to inhibit the current transient due to the addition of ATP in the absence of K^+ (Van der Hijden et al., 1990). Since there is no formation of acid in the aqueous phase of vesicles in the absence of K^+, it is conceivable that the presence of H^+ in the M5/M6 region due to formation of $E_2P{\cdot}H^+$ is sufficient to activate omeprazole in the bilayer conditions where there is virtually no aqueous space. This could result in binding of the sulfenamide at its site of formation, presumably at cysteine 813 and/or 822.

(*B*) *β Subunit.* Virtually no labelling of the β subunit by omeprazole was noted, although there are six cysteines predicted in the extracytoplasmic domain of this subunit. Since the sulfenamide does not react with disulfides, the most likely explanation is that the cysteines in this region of the β subunit are disulfide-linked. Further evidence for the disulfide nature of these bonds was the absence of F-MI labeling of the β subunit following the 1/4 tryptic digestion procedure but labeling after DTT reduction (data not shown). In the case of the β subunit of the Na^+,K^+-ATPase, it would appear that these conserved cysteines are also in the disulfide form (Kirley, 1989), another instance of the homology between the two pumps.

Stoichiometry of Labeling. The overall stoichiometry of labeling in these experiments was 2.2 ± 0.3 mol of omeprazole/mol phosphoenzyme, with a range of 1.7–3.4. It is therefore expected that at least two and perhaps three cysteines are able to react with the sulfenamide formed in the acid space of the vesicles. The labeling of intact enzyme was stable over several weeks when the enzyme was kept frozen. Following digestion, there was some loss of counts to the supernatant of the membrane pellet that corresponded to free reagent. After SDS gel separation, further counts were found at the bottom of the gel not retained by the PVDF membrane. Thus, after the enzyme is fragmented or solubilized in SDS (Lorentzon et al., 1987) the sulfenamide is apparently able to be displaced, most likely by other SH groups in the enzyme or enzyme fragments or by SH groups in the trypsin or trypsin fragments, since loss of counts was reduced in the presence of iodoacetamide or NEM treatment of the enzyme prior to digestion and gel separation. That only cysteines react with the sulfenamide is shown by the total removal of counts by mercaptoethanol.

The stoichiometry of labeling of the peptides separated on the gels after the progressive tryptic digestion appeared to be greater for those peptides containing cysteines 813 and 822 as compared to the peptides deriving from cysteine 892. This could be due either to more labeling of the former cysteines or labeling of both cysteines or greater loss from the label at cysteine 892 or a combination. The stoichiometry of labeling of sequences contained in the M5/M6 region was close to 1. Correcting for the loss of counts, the initial stoichiometry could be as high as 2 in this segment, arguing for reaction of both cysteines.

The stoichiometry of labeling of the peptides containing only cysteine 892 was about 0.4. With loss of 50% of the label, the initial stoichiometry at this site could be as high as 1. The final calculated stoichiometry based on the above reasoning would be close to 3 mol of omeprazole/mol of phosphoenzyme, the lower mean value of 2.2 being then due to some loss of label during the washing and precipitation procedure.

Figure 7 summarizes the above studies on the H^+,K^+-ATPase by presenting a working model of the membrane topology and of inhibitory binding sites. The linear amino acid sequence of the enzyme is displayed in terms of the membrane-spanning segments and the C-terminal domain. The tryptic cleavage sites described in this paper determined the arrangement shown of the membrane-spanning segments, and the three possible cysteines that react with omeprazole are shown as well as the $MeDAZIP^+$ site (Munson et al., 1991).

Inhibition of Acid Secretion. The location of the omeprazole sites at Cys^{813} or Cys^{822} and Cys^{892} defines the extracytoplasmic region of the α subunit targeted by this antiulcer drug. It must be binding to these cysteines that is responsible for the inhibition of acid secretion. It is known that the action of omeprazole is long-lasting; about 72 h is required for restoration of full acid secretion after stopping omeprazole administration is stopped (Larsson et al., 1985). This is readily explained by the reaction of omeprazole with the cysteines of the pump as described above. The reaction results in a stable covalent reaction product, which could only be reversed biologically by reaction with thiols.

The extracytoplasmic face of the pump apparently remains extracellular during its lifetime. The cysteines that react with

omeprazole are present in this domain. If they became exposed to the gluthathione of the cytosol, rapid reversal of acid secretory inhibition would be found. Since restoration of full acid secretion requires 72 h, reversal of omeprazole labeling in vivo most likely requires synthesis of new α subunits. It has been demonstrated that the protein synthesis inhibitor cycloheximide administered to rats prevents the reversal of omeprazole inhibition of acid secretion in vivo (Im et al., 1985). Since the lifespan of parietal cells averages 90 days, restoration of acid secretion is clearly related to pump biosynthesis, not cell turnover.

REFERENCES

Bamberg, K., Mercier, F., Reuben, M., Kobayashi, Y., & Sachs, G. (1992) *Biochim. Biophys. Acta* (in press).

Capasso, J. M., Hoving, S., Tal, D. M., Goldshleger, R., & Karlish, S. J. D. (1992) *J. Biol. Chem. 267*, 1150–1158.

Clarke, D. M., Loo, T. W., Inesi, G., & MacLennan, D. H. (1989) *Nature 339*, 476–478.

Clarke, D. M., Loo, T. W., & MacLennan, D. H. (1990) *J. Biol. Chem. 265*, 6262–6267.

Green, N. M. (1989) *Biochem. Soc. Trans. 17*, 970–972.

Hall, K., Perez, G., Sachs, G., & Rabon, E. (1991) *Biochim. Biophys. Acta 1077*, 173–179.

Im, W. B., Blakeman, D. P., & Davis, J. P. (1985) *Biochem. Biophys. Res. Commun. 127*, 78–82.

Kaminski, J. J., Bristol, J. A., Puchalski, C., Lovey, R. G., Elliott, A. J., Guzik, H., Solomon, D. M., Conn, D. J., Domalski, M. S., Wong, S., Gold, E. H., Long, J. F., Chiu, P. J. S., Steinberg, M., & McPhail, A. T. (1985) *J. Med. Chem. 28*, 876–892.

Keeling, D. J., Fallowfield, C., & Underwood, A. H. (1987) *Biochem. Pharmacol. 36*, 339–344.

Keeling, D. J., Taylor, A. G., & Schudt, C. (1989) *J. Biol. Chem. 264*, 5545–5551.

Kirley, T. L. (1989) *J. Biol. Chem. 264*, 7185–7192.

Lane, L. K., Kirley, T. L., & Ball, W. J., Jr. (1986) *Biochem. Biophys. Res. Commun. 138*, 185–192.

Larsson, H., Mattsson, H., Sundell, G., & Carlsson, E. (1985) *Scand. J. Gastroenterol. 108*, 79–94.

Lindberg, P., Nordberg, P., Brandstrom, A., & Wallmark, B. (1986) *J. Med. Chem. 29*, 1327–1329.

Lorentzon, P., Jackson, R., Wallmark, B., & Sachs, G. (1987) *Biochim. Biophys. Acta 897*, 41–51.

Lowry, O. H., Rosebrough, N. J., Farr, A. L., & Randall, R. J. (1951) *J. Biol. Chem. 193*, 265–275.

McLennan, D. H., Brandl, C. J., Korczak, B., & Green, N. M. (1985) *Nature 316*, 696–700.

Maeda, M., Ishizaki, J., & Futai, M. (1988) *Biochem. Biophys. Res. Commun. 157*, 203–209.

Matthews, I., Sharma, R. P., Lee, A. G., & East, J. M. (1990) *J. Biol. Chem. 265*, 18737–18740.

Mendlein, J., & Sachs, G. (1990) *J. Biol. Chem. 265*, 5030–5036.

Morii, M., Takata, H., & Takeguchi, N. (1990) *Biochem. Biophys. Res. Commun. 167*, 754–760.

Munson, K. B., Gutierrez, C., Balaji, V. N., Ramnayaran, K., & Sachs, G. (1991) *J. Biol. Chem. 266*, 18976–18988.

Nishikawa, K., & Oi, T. (1986) *J. Biochem. (Tokyo) 100*, 1043–1047.

Pedemonte, C. H., & Kaplan, J. H. (1990) *Am. J. Physiol. 258*, C1-23.

Price, C. E., & Lingrel, J. B. (1988) *Biochemistry 27*, 8401–8410.

Rabon, E., Sachs, G., Bassilian, S., Leach, C., & Keeling, D. (1991) *J. Biol. Chem. 266*, 12395–12401.

Reuben, M. A., Lasater, L. S., & Sachs, G. (1990) *Proc. Natl. Acad. Sci. U.S.A. 87*, 6767–6771.

Sachs, G., Chang, H. H., Rabon, E., Schackman, R., Lewin, M., & Saccomani, G. (1976) *J. Biol. Chem. 251*, 7690–7698.

Schagger, H., & von Jagow, G. (1987) *Anal. Biochem. 166*, 368–379.

Scott, D., Munson, K., Modyanov, N., & Sachs, G. (1992) *Biochim. Biophys. Acta* (in press).

Shin, J. M., Besancon, M., Simon, A., & Sachs, G. (1993) *Biochim. Biophys. Acta* (in press).

Shull, G. E. (1990) *J. Biol. Chem. 265*, 12123–12126.

Shull, G. E., & Lingrel, J. B. (1986) *J. Biol. Chem. 261*, 16788–16791.

Subrahmanyeswara-Rao, U., Hennessy, J. P., & Scarborough, G. A. (1991) *J. Biol. Chem. 266*, 14740–14746.

Van Der Hijden, H. T. W. M., Grell, E., De Pont, J. J. H. M., & Bamberg, E. (1990) *J. Membr. Biol. 114*, 245–256.

Wallmark, B., Larsson, H., & Humble, L. (1985) *J. Biol. Chem. 260*, 13681–13684.

Wallmark, B., Briving, C., Fryklund, J., Munson, K., Jackson, R., Mendlein, J., Rabon, E., & Sachs, G. (1987) *J. Biol. Chem. 262*, 2077–2084.

Yoda, A., & Hokin, L. E. (1970) *Biochem. Biophys. Res. Commun. 40*, 880–886.